FISEVIER

Contents lists available at ScienceDirect

Science of the Total Environment

journal homepage: www.elsevier.com/locate/scitotenv



A decision-making framework for the optimal design of renewable energy systems under energy-water-land nexus considerations



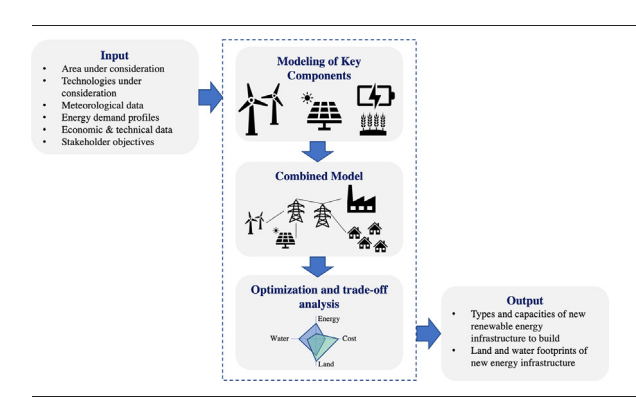
Julie Cook ^{a,b}, Marcello Di Martino ^{a,b}, R. Cory Allen ^{a,b}, Efstratios N. Pistikopoulos ^{a,b}, Styliani Avraamidou ^{c,*}

- ^a Artie McFerrin Department of Chemical Engineering, Texas A&M University, Jack E. Brown Chemical Engineering Building, 3122 TAMU, 100 Spence St., College Station, TX 77843, United States
- ^b Texas A&M Energy Institute, Texas A&M University, 1617 Research Pkwy, College Station, TX 77843, United States
- ^c Department of Chemical and Biological Engineering, University of Wisconsin-Madison, Madison, WI 53706, United States

HIGHLIGHTS

- Detailed models of key components of energy systems with water-land considerations
- Integrated optimization model for infrastructure planning of energy systems
- Multi-objective optimization approach for energy-water-land nexus trade-off analysis
- Derivation of cost power output surrogate models for renewable energy technologies

GRAPHICAL ABSTRACT



ARTICLE INFO

Article history:
Received 30 December 2021
Received in revised form 23 February 2022
Accepted 23 February 2022
Available online 1 March 2022

Editor: Huu Hao Ngo

Keywords:
Renewable energy
Energy storage
Multi-scale optimization
Mixed-integer linear optimization
Energy systems engineering

ABSTRACT

The optimal allocation of land for energy generation is of emergent concern due to an increasing demand for renewable power capacity, land scarcity, and the diminishing supply of water. Therefore, economically, socially and environmentally optimal design of new energy infrastructure systems require the holistic consideration of water, food and land resources. Despite huge efforts on the modeling and optimization of renewable energy systems, studies navigating the multi-faceted and interconnected food-energy-water-land nexus space, identifying opportunities for beneficial improvement, and systematically exploring interactions and trade-offs are still limited. In this work we present the foundations of a systems engineering decision-making framework for the trade-off analysis and optimization of water and land stressed renewable energy systems. The developed framework combines mathematical modeling, optimization, and data analytics to capture the interdependencies of the nexus elements and therefore facilitate informed decision making. The proposed framework has been adopted for a water-stressed region in south-central Texas. The optimal solutions of this case study highlight the significance of geographic factors and resource availability on the transition towards renewable energy generation.

1. Introduction

Global population is projected to continuously increase (Gu and Andreev K, 2021), and with that comes an increased demand for energy,

food, water and land (Garcia and You, 2016; Vakilifard et al., 2018). Land is becoming a scarce resource in many countries, which gives rise to the need for more efficient land use allocation both for food and energy production (Lambin and Meyfroidt, 2011). Furthermore, water usage has been

E-mail addresses: julie98cook@tamu.edu (J. Cook), dimartino@tamu.edu (M. Di Martino), rcallen24@tamu.edu (R.C. Allen), stratos@tamu.edu (E.N. Pistikopoulos), avraamidou@wisc.edu (S. Avraamidou).

^{*} Corresponding author.

growing globally at more than twice the rate of population (Boretti and Rosa, 2019; United Nations, 2019). Moreover, an increasing number of regions have reached the limit at which water services can be sustainably delivered, especially in arid regions such as Texas (Di Martino et al., 2021). Consequently, achieving food, energy, and water security in the future, while using resources in a sustainable manner is a major challenge we need to address (Avraamidou et al., 2020; Baratsas et al., 2021).

The conventional fossil-based energy provision systems are water intensive and responsible for the majority of global greenhouse gas (GHG) emissions (Bogdanov et al., 2021). A transition towards renewable energy generation could result in providing universal access to clean and affordable energy, reduce GHG emissions, and also decrease water scarcity by eliminating freshwater usage in thermal power plants (Lohrmann et al., 2019). Although, this transition comes with many challenges. Renewable energy sources, such as wind and solar, are inconsistent throughout the day as well as seasonally and spatially. This presents the need for large capacity storage systems to store the intermittent renewable energy for use during low sunlight or wind hours (Allen et al., 2021, 2022; Joskow, 2019). Furthermore, renewable energy generation tends to be much less energy dense than fossil-based methods, requiring much more land area to produce the same amount of energy (Nie et al., 2019a). Another challenge is that growing crops to use for bio-energy requires a large amount of water and land resources (Drews et al., 2020). Therefore, even though renewable energy systems do not have the same environmental impact as fossil fuel based methods, they can still place huge stresses on food, land and water resources, especially in semi-arid areas.

To tackle these challenges, a holistic food-energy-water-land nexus approach needs to be followed to systematically evaluate the interdependence and trade-offs of different renewable energy system solutions (Finley and Seiber, 2014). That is, for the energy system optimization problem, solutions considering the scope of the nexus rather than the individual food, energy, water, and land elements would provide more environmentally and socially sustainable decisions due to the very nature of the interconnected nexus in renewable energy systems. Many challenges emerge when considering nexus wide decision-making approaches, including: (i) the identification and modeling of interactions among nexus elements; (ii) the solution of the highly complex and interconnect nexus system models; (iii) the multiple, often conflicting stakeholder interests and objectives; and (iv) the choice of system boundaries. Therefore, typically only two of the interconnected nexus elements receive direct study due to the complexities that can arise in the multi-faceted, multispatial and multi-temporal nexus systems (Garcia and You, 2016), with the energy-water nexus being well studied for renewable energy systems (Allen et al., 2019; Chen et al., 2021; Martín and Grossmann, 2015; Di Martino et al., 2020; Garcia and You, 2015).

Current methodologies used in nexus studies mainly include dataintensive modeling and life cycle analysis for specific technologies or products (Albrecht et al., 2018). These approaches can provide some essential knowledge and are useful for expanding our understanding of foodenergy-water-land nexus interactions and addressing social and economic concerns of energy systems under nexus considerations. Although, to achieve a quantitative understanding of the multi-faceted interconnected nexus systems and make technically, environmentally and socially optimal decisions for renewable energy infrastructure, it is required to holistically solve modeling and data challenges using appropriate predictive modeling approaches (Nie et al., 2019b), effective integration of data and models at different scales (Demirhan et al., 2021; Biegler and Lang, 2012), mathematical optimization of trade-offs (Di Martino et al., 2022; Pappas et al., 2021; Avraamidou et al., 2018a), and generic metrics for assessing nexus interconnections in the system (Mohtar and Daher, 2019; Avraamidou et al., 2018b; Baratsas et al., 2022).

The tools and approaches developed by the Process Systems Engineering research community can aid in the solution of the aforementioned challenges, with a number of recent developments tackling the food-energy-water nexus through multi-scale modeling, optimization and trade-off analysis (Garcia and You, 2016; Namany et al., 2021; Nie et al., 2019a; Gao et al., 2021; Garcia and You, 2017; Ahmetovic et al., 2010; Beykal et al., 2020).

In this work, a multi-scale mathematical modeling and optimization framework is developed, capable of holistically addressing energy-waterland nexus interactions in renewable energy systems, and therefore facilitating informed land use allocation decisions for new renewable infrastructure developments. The proposed framework can determine the optimal mix of renewable energy generation and storage systems under different scenarios and objectives, including cost, energy production, water use and land use. The types of solutions generated by the proposed framework include the optimal type and size of energy storage and generation units in order to meet a specified energy demand profile over the course of a given time period. The proposed framework utilizes multi-scale energy systems engineering approaches, along with data analytics and hybrid modeling to capture nexus interactions and uncertainties to facilitate decision making for land-use allocation.

The remainder of this paper is structured as follows: the next section defines the problem under consideration; Section 3 describes the developed framework and the methodology used for its derivation; Section 4 introduces the Amarillo-Texas case study and presents results for different supply and demand scenarios; and finally Section 5 concludes this work.

2. Problem definition

This work presents a generic framework to optimize the trade-offs in terms of the energy-water-land nexus for the selection, design and allocation of renewable energy systems. To define the system under consideration the set of energy sources, energy conversion technologies, and energy storage technologies locally available, along with energy demand profiles to be satisfied, need to be specified. This is represented in Fig. 1 where an example of different technological options is illustrated. Furthermore, the available land and water resources also need to be specified along with weather data. Using this information the developed framework is able to identify the best mix of energy generation and storage technologies, their capacity, and water and land use.

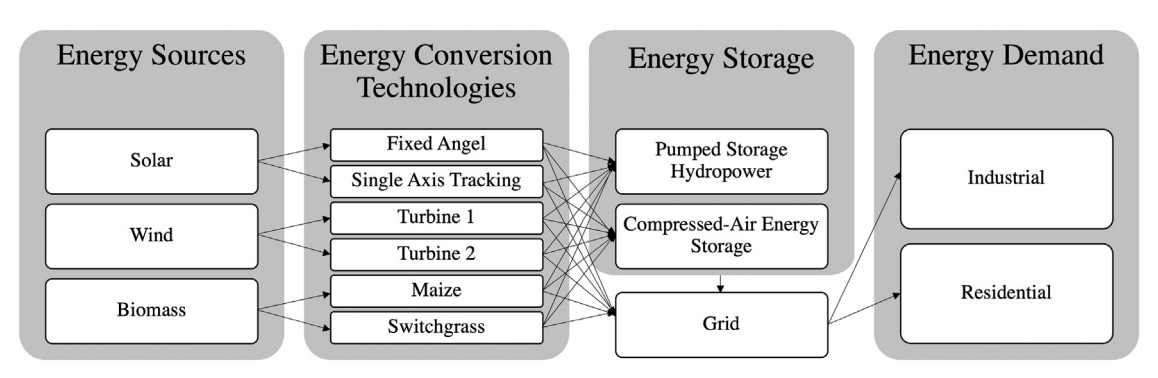


Fig. 1. Representation of the alternative pathways that can be considered by the developed framework.

In this framework, based on stakeholder interest and feedback, the optimization objectives include: (i) the total cost; (ii) the total water use; and (iii) the total land use of the renewable energy system under consideration.

As shown in Fig. 1, we can consider different types of solar panels, wind turbines and biomass for the energy generation along with different types of energy storage devices, to fulfill different energy demand profiles (e.g. for a residential area, or a neighborhood).

The input data in the developed renewable energy system model include input water, solar irradiance and wind resources, as well as economic data from social surveys and governmental reports. The alternative technological pathways can be identified based on local resource availability.

This work uses Amarillo, TX, USA as a case study to illustrate and elaborate on the developed framework. In Amarillo, renewable energy sources in the form of wind and solar are plentiful. Furthermore, land for potential wind and solar farms or biomass cultivation is generally available for purchase. However, many areas in Texas frequently experience drought conditions, so water usage is an important factor to be considered (Scanlon et al., 2013).

3. Framework for the optimal allocation of renewable energy systems under energy-water-land nexus considerations

Fig. 2 summarizes the developed framework that includes two main parts: (i) the modeling of the key components of the energy system; and (ii) their integration into a holistic energy system model.

The first step involves the collection of local resource data, including historic weather data (solar irradiance, wind speeds, etc.), land prices, and infrastructure costs. Detailed models for each energy generation

technology are then built based on the input data. The generated data is used in the third step to develop surrogate models of the complex and detailed key component models generated in the previous step. The surrogate models along with other constraints and considerations are merged in a combined mixed-integer linear programming (MILP) model in step 4 that integrates all alternative energy generating processes into a holistic optimization problem. The last step of the framework is the analysis of different resource and demand scenarios under multiple objectives (cost minimization, water use minimization, land use minimization and energy demand fulfillment).

The following subsections are describing in more detail the framework steps and the derived mathematical models.

3.1. Modeling of key components of the energy system

In the following, the modeling steps for solar farms, wind farms, biomass and energy storage are discussed in detail.

3.1.1. Solar farm modeling

Two panel setup options are considered for the solar farm modeling: fixed angle, and single axis tracking panels. Fixed angle panels are stationary, while single axis tracking panels change their tilt angle with a motorized system to improve efficiency by tracking the movement of the sun throughout the day. To develop the solar farm model, firstly the optimal panel/inverter combination was determined for both fixed and single axis tracking panels, and then an optimization model was solved for different power outputs to develop power vs. cost and land correlations. The PVLIB Toolbox for Python, developed by Sandia National Laboratories (Holmgren et al., 2018), was used for both these steps as a black box solver

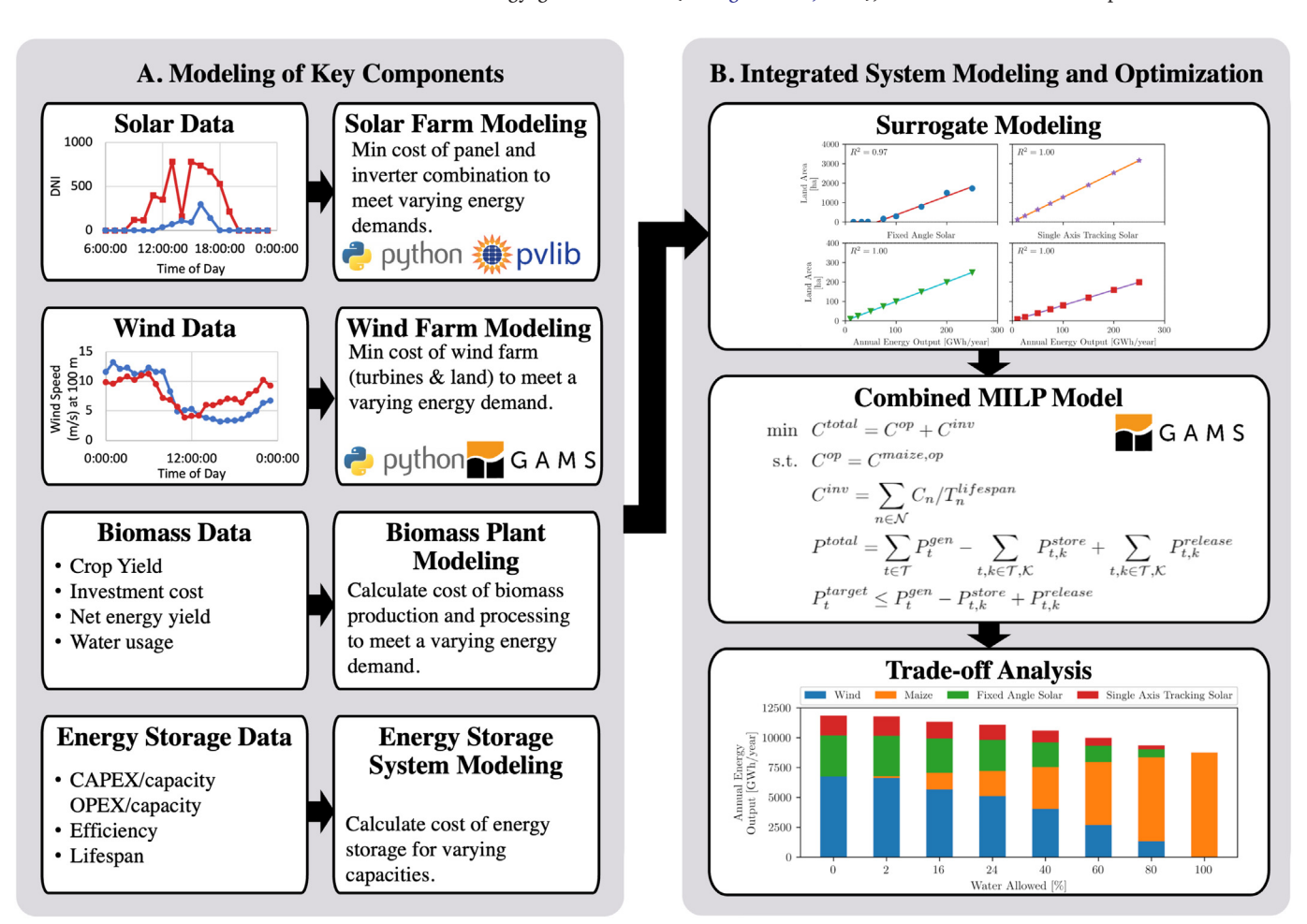


Fig. 2. Framework overview with relevant modeling steps.

to convert solar irradiance data measured at hourly intervals into power outputs. PVLIB is a collection of methods and modeling techniques developed by Sandia National Laboratories for the performance of photovoltaic (PV) projects. This includes a library of available technologies and their associated specifications, conversion of solar irradiance to power output, and tracking abilities of single axis tracking systems.

To determine the optimal solar panel and inverter combination, a model was created to maximize the power output of each combination by varying the tilt (θ) and azimuth direction (ϕ) for the fixed angle panels. For the single axis tracking panels, the azimuth (ϕ) was the only optimization variable as the time-dependent tilt angle was already optimized by the black box solver. The objective functions for the fixed angle and single axis tracking are summarized in Eqs. (1) and (2), respectively.

$$\max_{x \in X} \left\{ \frac{1}{area\left(\mathbf{x}\right) \max_{\theta, \phi} power\ output\left(\mathbf{x}, \theta, \phi | solar\ data\right)} \right\}$$
 (1)

$$\max_{x \in X} \left\{ \frac{1}{area(x) \max_{\phi} power \ output(x, \phi | solar \ data)} \right\}$$
 (2)

In these cases, $x \in X$ denotes the set of analyzed panel and inverter combinations. Consequently, the power output was normalized by the area of each solar panel (area(x)) and the results were compared with the costs of a large scale implementation of these pairs. The highest power output pair of panel and inverter was also the lowest cost system, so this pair was selected to advance to the next stage of the modeling. Were this not the case, further analysis may have been necessary to determine the optimal pair.

Using the selected pair of panel and inverter, an optimization model was developed to minimize the cost of a solar farm system capable of meeting a discrete set of yearly power demands. The same model framework was used for both fixed angle and single axis tracking panels with different inputs for power outputs that were calculated by PVLIB, required area, and costs. The objective function and critical constraints for this modeling step are shown below.

$$\min C^{total} = C^{panels} + C^{land} \tag{3}$$

$$s.t.C^{panels} = C^P \cdot N \tag{4}$$

$$C^{land} = A \cdot N \cdot C^L \tag{5}$$

$$A = A^{panel} \cdot cos\theta + L^{spacing} \cdot L^{panel} \tag{6}$$

$$N = \frac{pd}{PO} \tag{7}$$

$$C^{P} = \kappa_{plant} \cdot f_{NREL} \tag{8}$$

$$\kappa_{plant} = N \cdot P$$
(9)

The total system cost (Eq. (3)) is minimized according to the panel (Eq. (4)) and land cost (Eq. (5)). The area of one solar panel is derived based on the panel area itself, as well as the necessary spacing between neighboring panels (Eq. (6)). Here, pd denotes the power demand to be satisfied by the solar farm, whereas PO specifies the power output of a single panel as defined by PVLIB. Accordingly, Eq. (7) calculates the number of panels. Further, P defines the capacity of a single panel based on PVLIB, whereas f_{NREL} summarizes all solar panel costs except land costs, based on Fu et al. (2018). Therefore, the cost of a single panel can be derived with Eq. (8), whereas the solar farm capacity can be determined with Eq. (9). The output costs from this model were used with the set of power demands (pd) to create Pareto curves for both fixed angle and single axis tracking

panel systems. These relationships between cost, land and power output are then used as inputs for the integrated model.

3.1.2. Wind farm modeling

The optimization model of the wind farms involves the minimization of the cost of meeting a range of yearly energy demands using only wind turbines. The number of turbines and the spacing between them were optimized. The developed wind farm model includes some nonlinear terms, including the cost equations and the effect of turbulence on wind speed, resulting in the model being a mixed integer nonlinear programming (MINLP) model. The developed MINLP model is presented in Eqs. (10) to (42).

The power output of the wind turbines was modeled using piecewise linear approximations of the power generation profile of the selected turbine(s). The power output was assumed zero below cut in speed and above cut out speed. Additionally, the power output was approximated to be linear from zero to its max value from the cut in speed to the rated speed, and was approximated to be constant at its max value from the rated speed to the cut out speed. All of the above factors were combined into a MINLP model, which was solved in GAMS¹ with the BARON² solver (Sahinidis, 1996) for a range of energy demands. The objective function and critical constraints for the wind farm model are shown below (Eqs. (10) to (42)).

The total wind farm cost is minimized (Eq. (10)) based on the turbine cost (Eq. (11)) and the land cost (Eq. (12)), while the desired power demand is fulfilled according to Eqs. (13) and (14). Here, $y_c^{t, op}$, $_t$ is a binary variable specifying if a turbine is in operation in column position c, in row position r, on representative day n at time t.

$$\min C^{total} = C^{turbine} + C^{land} \tag{10}$$

$$s.t.C^{turbine} = N^{turbine} \cdot C^{emp} \tag{11}$$

$$C^{land} = A \cdot C^L \tag{12}$$

$$p^{total} \ge P^{demand}$$
 (13)

$$p^{total} = \sum_{c,r,n} po_{c,r,n,t}^{act} \cdot y_{c,r,n,t}^{t,op}$$

$$\tag{14}$$

The cost of a turbine was determined through empirical equations derived by Fingersh et al. (2006). Each component of the turbine has its own cost that depends on the specifics of the turbine, such as size and technology utilized, as well as additional costs, such as engineering and permitting. Finally, the cost was adjusted to current dollars from the 2002 values in the NREL report (Fingersh et al., 2006). Eq. (15) represents these empirical cost correlations together with an inflation index that are used as the basis of determining the turbine cost. The set $u \in U = \{\text{blade}, \text{hub}, \text{pitch}, \text{nose}, \text{shaft}, \text{bearing}, \text{brake}, \text{elec}, \text{yaw}, \text{cool}, \text{nac}, \text{safety}, \text{tower}, \text{found}, \text{int}, \text{gearbox}, \text{gen}, \text{main}, \text{platform}, \text{trans}, \text{road}, \text{install}, \text{permit}\}$ summarizes all considered cost components of the wind turbine. As representative examples, the installation cost (Eq. (16)) and blade cost functions (Eq. (17)) are shown below.

$$C^{emp} = 1.4235 \cdot \sum_{u} C_u \tag{15}$$

$$u = \text{`install'} : C_{install} = 1.965 \cdot HD^{1.1736}$$
 (16)

$$u = \text{`blade'}: C_{blade} = 2.16 \cdot ((0.4019R^3 - 955.24) + 2.7445R^{2.5025})$$
 (17)

¹ General Algebraic Modeling System (GAMS) is a high level modeling system for mathematical programming and optimization. It consists of a language compiler and a range of associated solvers.

 $^{^2\,}$ BARON is a mathematical optimization solver that uses a branch-and-reduce algorithm. BARON can search for global solutions of mixed-integer nonlinear problems.

The radius (R) and the rotor area (A_{rot}) are calculated with the following two equations. These values need to be mainly determined for the empirical cost correlations and the wind speed adjustment calculations.

$$R = 0.5 \cdot D \tag{18}$$

$$A_{rot} = \pi R^2 \tag{19}$$

Moreover, Eqs. (20) and (21) enforce that only one gearbox and generator technology can be selected.

$$\sum_{gb} y_{gb} = 1, gb \in GB = \{0, 1, 2, 3\}$$
 (20)

$$\sum_{gen} y_{gen} = 1, gen \in GEN = \{0, 1, 2, 3\}$$
 (21)

Eqs. (22) to (24) load the necessary wind speed data from an external file, and adjust it according to the height difference between the measurement height and the hub height (Xu et al., 2018), as well as consider the changes in wind speeds due to turbine spacing (Attias and Ladany, 2011).

$$\nu'_{n,t} = \nu^0_{n,t} (H/100)^{0.15} \tag{22}$$

$$\nu_{r1',n,t} = \nu'_{n,t} \tag{23}$$

$$\nu_{r,n,t} = \nu'_{n,t} \cdot \left(1 - \left(\frac{\nu_{r-1,n,t}}{3 \cdot \left(\nu'_{n,t} + 0.0001 \right)} \right) \right) \cdot \left(\frac{R}{R + 0.078 \cdot x} \right)^2 \right) \tag{24}$$

Then, the numbers of turbines in each column and row are counted (Eqs. (25) and 26). Here, $y_c^{t, \, bay}$ is a binary decision variable for turbine purchasing. The overall required area can be calculated with Eq. (27), while a selected ratio between columns and rows can be incorporated (Eq. (28)). The overall number of wind turbines can be derived with Eq. (29).

$$N_c = \sum_{c,'r1'} t_{c,'r1'}^{t,buy} \tag{25}$$

$$N_r = \sum_{r} y_{r_c 1', r}^{t, buy} \tag{26}$$

$$A = x^2 \cdot N_c \cdot N_r \tag{27}$$

$$N_c = 2 \cdot N_r \tag{28}$$

$$N^{turbine} = \sum_{c,r} y_{c,r}^{t,buy} \tag{29}$$

Furthermore, Eq. (30) ensures that a turbine can only be operating when it is also purchased, whereas Eqs. (31) and (32) enforce that neighboring turbines upstream have to be in operation when the downstream turbine is operating.

$$y_{c,r,n,t}^{t,op} \le y_{c,r}^{t,buy}, \forall c, r, n, t \tag{30}$$

$$y_{c,r+1,n,t}^{t,op} \le y_{c,r,n,t}^{t,op}, \forall c, r, n, t$$
 (31)

$$y_{c+1,r,n,t}^{t,op} \le y_{c,r,n,t}^{t,op}, \forall c, r, n, t$$

$$\tag{32}$$

A constraint ensuring that the actual power output of a turbine is always less or equal than the power output derived with the turbine specific wind vs. power output profile is shown in Eq. (33). Further, a big-M constraint establishing the logical connection between the binary decision variable for turbine operation and actual power output is added (Eq. (34)).

$$po_{c,r,n,t}^{act} \le po_{c,r,n,t}, \forall c, r, n, t \tag{33}$$

$$po_{c,r,n,t}^{act} \le M \cdot y_{c,r,n,t}^{t,op}, \forall c, r, n, t$$
(34)

The power output of a turbine is derived based on a piecewise linear correlation incorporating the actual wind speed, as well as the turbine specific cut in speed, cut out speed, nominal speed and nominal power output, as stated from Eqs. (38) to (42) taking into account the slope of the wind speed vs. power output profile m (Eq. (35)), and the axis intercept b (Eq. (36)), together with the auxiliary wind speed variable $f_{i, c, n, r, t}$ (Eq. (37)). Further, in Eq. (39) the binary variable $z_{i, c, r, n, t}$ is introduced to ensure that only one section of the piecewise linear correlation can be selected for each turbine in column c, row r, at representative day n and time t.

$$m = p^n / (\nu^n - \nu^{ci}) \tag{35}$$

$$b = -p^n \nu^{ci} / (\nu^n \nu^{ci}) \tag{36}$$

$$\nu_{r,n,t} = \sum_{i} f_{i,c,r,n,t} \tag{37}$$

$$po_{c,r,n,t} = m \cdot f_{i2,c,r,n,t} + b \cdot z_{i2,c,r,n,t} + p^n \cdot z_{i3,c,r,n,t}$$
(38)

$$\sum_{i} z_{i,c,r,n,t} = 1 \tag{39}$$

$$0 \le f_{i1,c,r,n,t} \le \nu^{ci} \cdot z_{i1,c,r,n,t} \tag{40}$$

$$\nu^{ci} \cdot z_{i2,c,r,n,t} \le f_{i2,c,r,n,t} \le \nu^n \cdot z_{i2,c,r,n,t} \tag{41}$$

$$\nu^{n} \cdot z_{i3,c,r,n,t} \le f_{i3,c,r,n,t} \le \nu^{co} \cdot z_{i3,c,r,n,t}$$
(42)

With this large nonlinear mixed integer program, it was necessary to reduce the number of days simulated to make the problem tractable. Therefore, a year's worth of real wind speed data from the location under consideration was reduced to four representative days through k means clustering (Tso et al., 2020). K-means clustering is a machine learning algorithm and aims to find groups in a set of data, with the number of groups represented by the variable K. The algorithm works iteratively to assign each data point to one of K groups based on the features that are provided. Data points are clustered based on feature similarity. In this case K-means clustering was used to generate 4 clusters of days that have similar wind speeds. The four representative days selected are presented in Fig. 3.

The wind speed inputs to the model determined by k means clustering were adjusted from the measured height to the hub height of the selected turbine. The wind speed also had to be adjusted for any turbulence caused by surrounding turbines (Attias and Ladany, 2011). Fig. 4 demonstrates the amount of wind speed reduction for different cases of turbine spacing. The turbulent effect is much greater as the spacing between the turbines decreases. This highlights an important trade off determined by the model, which is that the additional spacing allows the turbines to be more efficient and less turbine purchases are required; however, the additional spacing also requires more land and therefore incurs a higher land cost.

The relationship between power output and cost can be approximated with a piecewise linear correlation. However, the model determined two distinct optimal turbine placement strategies, dependent on the number of turbines required to meet the demand. With fewer turbines, the model choses to arrange the turbines in a L-shaped pattern. This strategy does not fully utilize the purchased land; it instead spreads the turbines along the outside edges in order to minimize the effects of turbulence (see Fig. 5, green area). With a higher number of turbines, the cost of the non-utilized land was no longer worth the trade off for higher efficiency, so the model arranged the turbines in a grid pattern with more space between the turbines to use a different strategy for reducing turbulent effects and optimizing efficiency (see Fig. 5, blue area).

The model presented in Eqs. (10) to (42) was used to optimize wind farms with high energy loads. The objective function was changed to $\max P^{total}$ to optimize wind farms with lower energy loads, where the power output of a set number of turbines is maximized.

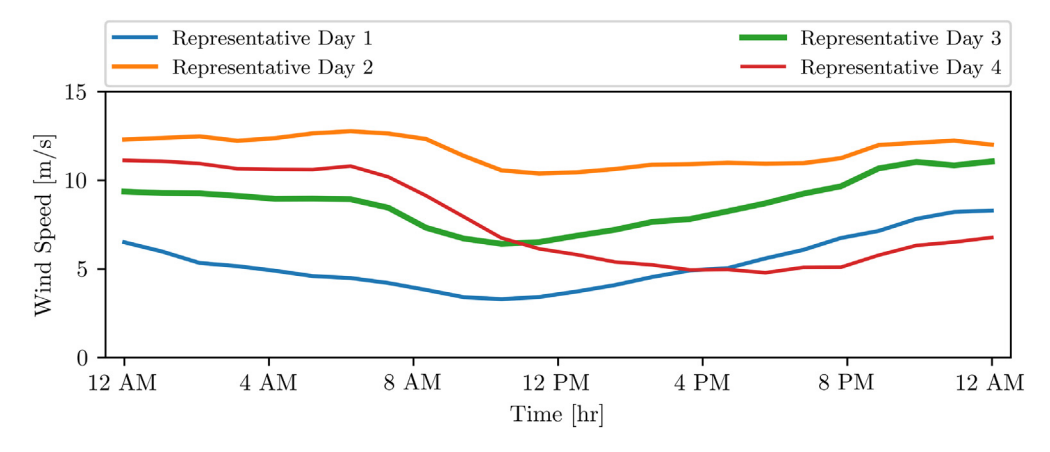


Fig. 3. Representative days for wind speeds resulting from K-means clustering.

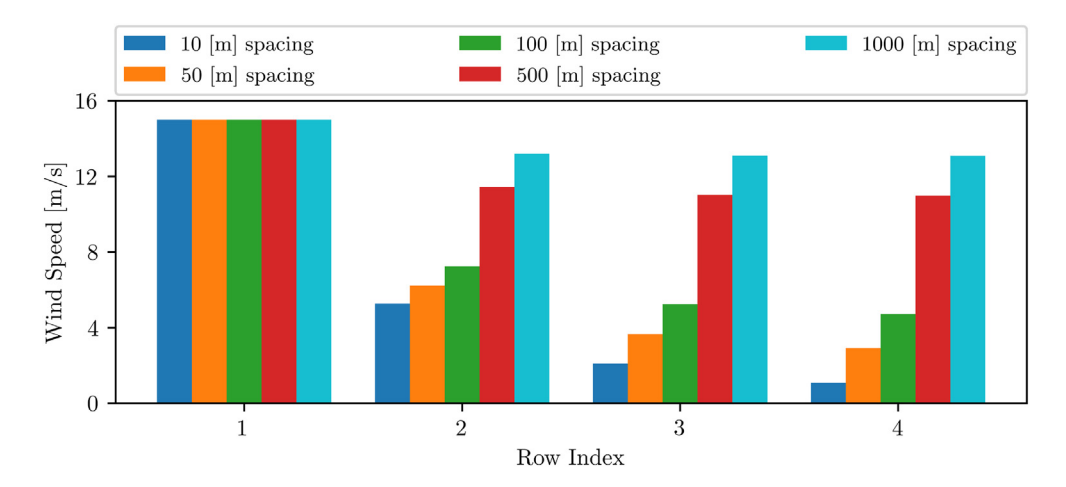


Fig. 4. Effect of turbine spacing on wind speed.

3.1.3. Biomass modeling

For biomass, the energy crop, maize, was assumed to be harvested throughout a year and converted through anaerobic digestion and gas treatment to pipeline quality biomethane that could be added to the natural gas grid. The biomethane was assumed to be available year round to combust in place of traditional natural gas. Using the yield of the crop (Lunik and Langemeier, 2015) and the net energy yield (Braun et al., 2010), the amount of energy available per unit area of crops was calculated. To develop an energy profile comparable to wind and solar, this amount of energy was distributed evenly across each hour of the year.

The relationship between the cost and energy output of a biomass processing system was determined using pricing figures for investment and

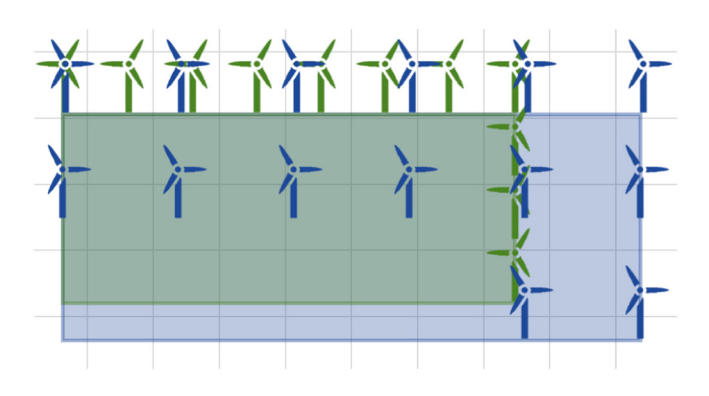


Fig. 5. L-shaped and grid configurations of wind turbines.

operating costs from Braun et al. (2010). The investment cost of the system depended on the required size of the digesting facility, while the operating cost depended on the amount of crop grown, harvested, and processed. The cost was then annualized based on an expected 15 year lifespan of the digesting facility.

The water used to irrigate the crops was also considered to account for water-stressed regions. The water requirements for growing and processing the energy crops are significantly higher than those for solar and wind systems, which were assumed to have negligible water requirements. The amount of water necessary depends on the type of crop as well as the climate of the area, as crops require more water when grown in warm, dry climates and less in cool, wet climates. For maize, the water requirements were assumed to be between 5000 and 8000 cubic meters per hectare per year.

3.1.4. Energy storage modeling

The dynamics of the energy storage systems under consideration are very fast and therefore were assumed to be instantaneous. Therefore, to add energy storage technology options to the model, solely information in terms of the capital and operational cost per capacity ($\frac{s}{kWh}$), the efficiency, and the lifespan have to be specified. Land and water use for energy storage devices were assumed to be negligible.

3.2. Integrated modeling and optimization

3.2.1. Surrogate models

A set of sample results of the modeling of key components step are summarized in Figs. 6 and 7. The sampling space was initially set to be between

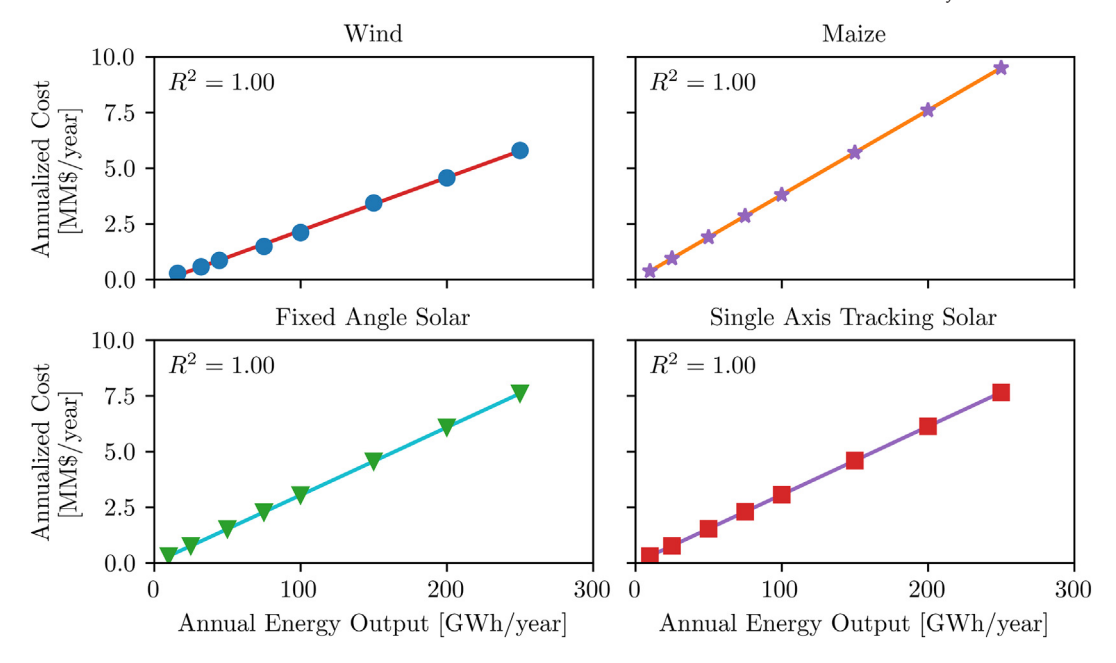


Fig. 6. Modeling of key components results - Energy output vs. annualized cost.

 $1\cdot 10^4 \frac{MWh}{year}$ and $2.5\cdot 10^5 \frac{MWh}{year}$. In the case of wind the lowest power output with a single turbine is derived to be $1.6\cdot 10^4 \frac{MWh}{year}$. Accordingly, the wind surrogate model has a slightly different value range. The sample results turned out to be sufficient for our optimization case studies, since the obtained results did not violate the yearly energy output range under investigation. Apart from that, the accuracy of the obtained fits are comparably high (for all cases $R^2 \geq 0.99$). Therefore, additional sampling is not necessary. However, if desired, i.e. one later obtained optimization solution is at the upper bound of the evaluated sampling range, further sampling points can easily be added and the obtained correlations updated. Firstly, all generated data was approximated with a linear correlation. If the obtained accuracy, in terms of the mean-square error (R^2) was not sufficiently high ($R^2 \geq 0.96$) a piecewise linear correlation is used instead. This modification was only employed for the wind case for the surrogate model capturing the correlation between power output and area, where two linear

correlations resulted in a sufficiently accurate fit $(R_1^2 = 0.965, R_2^2 = 0.975)$. If this were not the case a piecewise linear correlation with three sections would have been employed next and so on. The linear correlations for the presented wind case switch at $4.45 \cdot 10^4 \frac{MWh}{year}$. The accuracy of all generated approximations is also summarized in Figs. 6 and 7. The developed surrogates can be used in the integrated model so as to retain its linearity and tractability. These relationships were used to estimate the cost and land needs of the energy generating technologies considered by the integrated model. Additional costs incurred by energy storage were calculated from the ratings and capacities of the utilized storage technologies.

3.2.2. Combined MILP model

The linear surrogate models developed in the previous step are used to generate an integrated mixed-integer linear programming (MILP) model that can holistically describe the energy system and all applicable options.

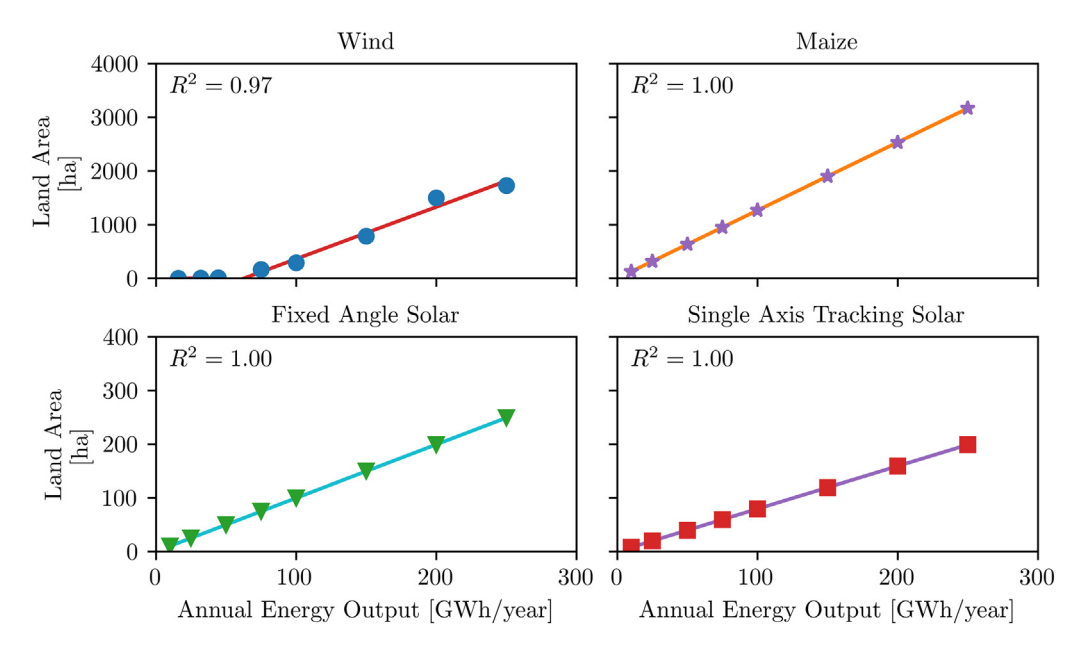


Fig. 7. Modeling of key components results - Energy output vs. area.

The integrated MILP model takes power outputs of one solar panel, one wind turbine, and 1 ha of crop land for biomass at hourly intervals, and scales each power output accordingly to meet an hourly power demand. The model has also the capability to optionally utilize energy storage technologies in order to meet the required energy demand. At each hour, the power generated from each technology can either be stored, released from the storage system, or directly outputted from the generating source to the electricity grid. In order to reduce land use, the model allowed for dual land use of growing biomass crops in between wind turbines. The objective of the model is to minimize cost; however, additional objectives, such as limiting area or water use, can also be considered. Overall, this results in an integrated MILP model as presented in Eqs. (43) to (77).

The objective function (Eq. (43)) minimizes the summation of both operating (C^{op}) and investment (C^{inv}) costs. Although, only the operating cost of maize is to be considered, since the operating cost of all other technologies can be neglected in comparison to their investment cost. Regarding investment cost, all generating and storage technologies are taken into account (Eq. (45)).

$$\min C^{op} + C^{inv} \tag{43}$$

$$s.t.C^{op} = C^{maize,op} \tag{44}$$

$$C^{inv} = \sum_{g \in G} \frac{C_g}{T_g^{lifespan}} + \sum_{k \in K} \frac{C_k}{T_k^{lifespan}}$$

$$\tag{45}$$

The total power balance is given in Eq. (46), whereas Eq. (47) ensures that in each time point at least P^{target} has to be available to satisfy the set power demand. Therefore, the generated power is calculated according to the available technologies in Eq. (48), based on the relevant power output data (Eq. (49)) and the respective number of used technologies (Eq. (50)).

$$P^{total} = \sum_{t \in T} P_t^{gen} - \sum_{t \in T, k \in K} P_{t,k}^{store} + \sum_{t \in T, k \in K} P_{t,k}^{release}$$

$$\tag{46}$$

$$P^{target} \leq P_{t}^{gen} - \sum_{t \in T, k \in K} P_{t,k}^{store} + \sum_{t \in T, k \in K} P_{t,k}^{release}, \forall t \in T$$
 (47)

$$P_t^{gen} = p_t^{scale_1} + p_t^{scale_2} + p_t^{scale_3} + p_t^{scale_4}, \forall t \in T$$

$$\tag{48}$$

$$P_t^{scale_g} = po_{g,t}, \forall g \in G \tag{49}$$

$$p_g = \sum_{s \in T} scale_g \cdot p_t^{scale_g}, \forall g \in G$$
 (50)

Then, the cost of the respective technologies can be calculated using the surrogate models according to Eqs. (51)–(55).

$$C_{solar} = 0.60765 \cdot p_1 + 0.61188 \cdot p_4 \tag{51}$$

$$C_{wind} = 0.45395 \cdot p_3$$
 (52)

$$C_{biomass} = 4440 \cdot p^{max, scale_2} \tag{53}$$

$$C_k = capex_k^c \cdot \kappa_k + capex_k^p \cdot P_k^{rat}, \forall k \in K$$
(54)

$$C^{maize,op} = 0.004221 \cdot p_2 \tag{55}$$

Regarding maize, Eq. (56) ensures that the correct overall power generation is calculated and Eq. (57) derives the amount of maize farming land. Further, the necessary land calculations are summarized in Eqs. (58) to (63). Eqs. (58) to (60) calculate the effective area difference between maize and wind to ensure the dual use land is not double counted. The water demand is calculated according to Eq. (64).

$$p^{\max,scale_2} \ge p_t^{scale_2}, \forall t \in T \tag{56}$$

$$scale_2 = A^{maize} (57)$$

$$A^{dif} = A^{wind} - A^{maize} (58)$$

$$A^{dife} \ge 0$$
 (59)

$$A^{dife} \ge A^{dif}$$
 (60)

$$A^{total} = A^{solar} + A^{wind} + A^{dife}$$

$$\tag{61}$$

$$A^{solar} = A^{sol,fixed} \cdot p_1 + A^{sol,SAT} \cdot p_4 \tag{62}$$

$$A^{wind} = \sum_{j \in J} slope_j \cdot pa_j + int_j \cdot z_j$$
 (63)

$$water^{total} = 7000 \cdot scale_2 \tag{64}$$

Eqs. (65) to (70) summarize the piecewise linear correlations that are used in Eq. (63) to calculate the necessary land based on the desired power output. Eq. (65) ensures only one piecewise section is selected while Eq. (66) sums the power output from each section, which is zero if not selected. Eqs. (67) to (70) establish the boundaries of the piecewise sections.

$$\sum_{i \in I} z_j = 1 \tag{65}$$

$$p_3 = \sum_{i \in J} pa_j \tag{66}$$

$$0 \le pa_{i1}$$
 (67)

$$pa_{i1} \le 4.5 \cdot 10^7 \cdot z_{i1}$$
 (68)

$$4.500001 \cdot 10^7 \cdot z_{j2} \le pa_{j2} \tag{69}$$

$$pa_{2} \le 2.5 \cdot 10^{10} \cdot z_{2}$$
 (70)

Lastly, the energy storage power balance, the energy storage power rating and capacity constraints, together with begin and end of life constraints are summarized from Eqs. (71) to (77). Eq. (71) ensures energy balancing at each time period. Eqs. (72) and (73) ensure the energy storage system does not release or store more power than it is rated for, while Eq. (74) enforces that the stored energy does not exceed the capacity of the system. Eq. (75) sets a minimum amount of energy that must remain in storage, and Eq. (76) ensures the amount of energy stored at the end of the time period is not less than the beginning balance.

$$P_{t,k}^{bat} = P_{t-1,k}^{bat} + P_{t,k}^{store} - P_{t,k}^{release}, \forall k \in K \& t \in T$$

$$\tag{71}$$

$$P_k^{rat} \ge P_{t,k}^{store}, \forall k \in K \& t \in T$$

$$\tag{72}$$

$$P_k^{rat} \ge P_{t,k}^{release}, \forall k \in K \& t \in T$$

$$\tag{73}$$

$$P_{t,k}^{bat} \le \kappa_k, \forall k \in K \& t \in T \tag{74}$$

$$P_{tk}^{bat} \ge 0.05 \cdot \kappa_k, \forall k \in K \& t \in T \tag{75}$$

$$\sum_{k \in K} P_{18760,k}^{bat} \ge \sum_{k \in K} P_{11,k}^{bat} \tag{76}$$

$$P_{t|,k}^{release} \le P_{t|,k}^{bat}, \forall k \in K \tag{77}$$

For $G = \{\text{solar fixed angle, solar single axis tracking, biomass, wind}\}$, $T = \{1,2,...,8760\}$, $K = \{PHS, CAES\}$ and $T_{solar}^{lifespan} = T_{wind}^{lifespan} = 20 \text{ years, } T_{biomass}^{lifespan} = 15 \text{ years, } T_{phss}^{lifespan} = 50 \text{ years, } T_{cAES}^{lifespan} = 30.$

3.2.3. Multi-objective optimization approach

Multi-objective optimization is used to simultaneously optimize cost, water use and land use. The ϵ -constraint method was used to generate

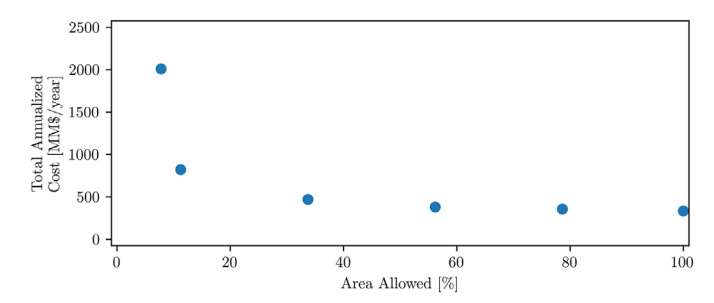


Fig. 8. Total annualized cost vs percent area allowed.

Pareto optimal solutions (Pappas et al., 2021), by expressing the land use and water use objectives as constraints.

To investigate the water use objective, Eqs. (78) and (79) are added to the combined MILP (Eqs. (44) to (77)).

$$Water^{total} \le Water^{max}$$
 (78)

$$Water^{max} = P^{target} \cdot ratio_{we} \tag{79}$$

Here, $ratio_{we}$ denotes the maximum water use to energy output ratio (m³ per kWh), e.g. 500 m³/kWh, and is varied to investigate the influence on limited water use on the energy mix.

To investigate the land use objective, Eqs. (80) and (81) are added to the combined MILP (Eqs. (44) to (77)).

$$A^{total} \le A^{max} \tag{80}$$

$$A^{max} = P^{target} \cdot ratio_{ae} \tag{81}$$

In this case, $ratio_{ae}$ determines the maximum land area use to energy output ratio (ha per kWh), e.g. 0.00692 ha/kWh.

Additionally, the equation $A^{dife} \ge 0$ is replaced with the following equations:

$$M \cdot y_m \ge A^{dif} \tag{82}$$

$$M \cdot y_m \le A^{dife} \tag{83}$$

$$A^{dif} \le A^{dif} \tag{84}$$

Subsequently, similar to $ratio_{we}$, $ratio_{ae}$ is varied to investigate the influence of limited land use on the energy mix.

The integrated multi-objective model was solved in GAMS using the CPLEX solver.

4. Case study - renewable energy system design in Amarillo, TX

To demonstrate the model, a case study was performed for the design of an energy system in Amarillo, Texas. The population in Texas is rapidly increasing, and with that comes an increased demand for energy. The current electrical grid in Texas relies heavily on fossil fuels, which create harmful emissions. Therefore, fossil fuels alone will not be a desirable energy option in the future. Renewable energy resources must be integrated into the grid in order to meet the energy demands for a growing population while reducing the environmental impact that comes from burning fossil fuels (Energy Reliability Council of Texas, 2018). In Amarillo, renewable energy sources in the form of wind and solar are plentiful. Furthermore, land for potential wind and solar farms or biomass cultivation is generally available for purchase. However, this region is highly water stressed. To illustrate the capabilities of the developed framework and show the effect of these geographic factors, two scenarios were considered: one land and one water constrained scenario.

The solar and wind speed data used in this case study were obtained from NREL for Amarillo, Texas in year 2015 (Fu et al., 2018).

4.1. Land constrained scenario

To evaluate the trade-offs between cost and land use, the area of land use allowed was varied from the maximum land (corresponding to the case when land use was not a constraint), to the minimum of 8% of the maximum land use. This resulted in the generation of the Pareto front presented in Fig. 8, that presents the effect of limited area on cost. As the area allowed became more restricted, the minimum total cost to meet the required energy demand increased drastically.

The breakdown of the technologies used at each area limitation is shown in Fig. 9, whereas Fig. 10 illustrates the land area used by each generating technology.

When the model is not constrained by area, it chooses to meet the energy demand entirely through biomass. The reason being that biomass is the only generating technology that does not require energy storage, allowing for cost savings. However, biomass requires the most land area. So as the area becomes less available, the model must choose other more expensive options to meet the energy demand within the constraints.

At the extreme cases of 8 and 11% area allowed, the model chooses single axis tracking solar panels because they require the least amount of area for the amount of energy output. These cases point out an interesting trade off the model can make. In the 11% scenario, the model chooses to buy more solar panels in order to avoid requiring large amounts of expensive energy storage. In the 8% scenario, there is not enough area for additional

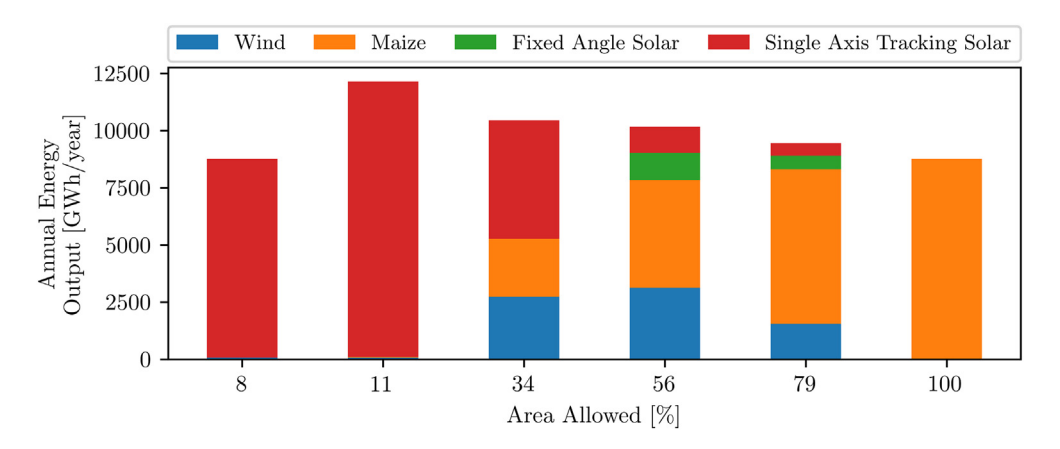


Fig. 9. Technology allocations at varying percentages of allowed area.

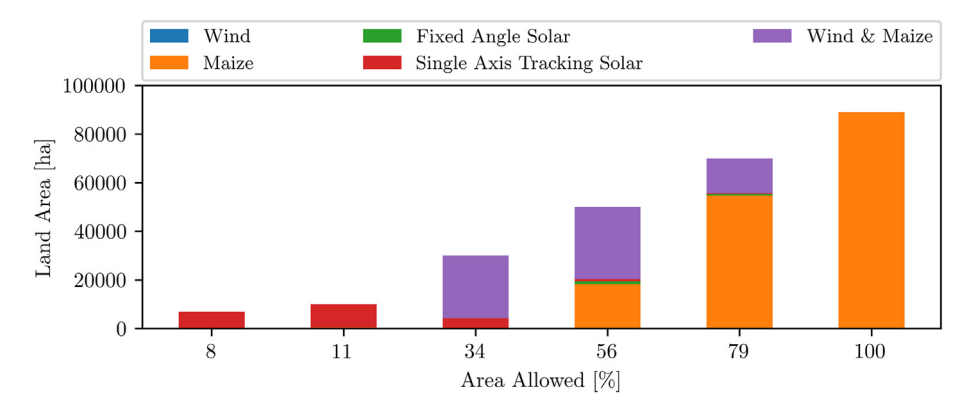


Fig. 10. Area allocation per generating technology.

panels, so additional storage capacity is required to stay within area restrictions.

4.2. Water constrained

To evaluate the trade-offs between cost and water use, the amount of water use allowed was varied from the maximum water usage (corresponding to the case when water use was not a constraint), to the minimum of zero water usage. This resulted in the generation of the Pareto front presented in Fig. 11, that presents the effect of limited water use on the cost of the energy system. As water use became more restricted, the total cost of the system increased, however, not as drastically as the land restricted case.

The breakdown of the technologies used at each water limitation is shown in Fig. 12.

When the model is not constrained by water, it chooses to utilize only biomass to meet the energy demand. This is for the same reason as the

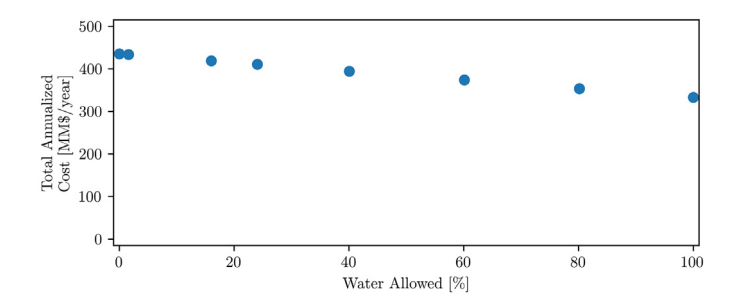


Fig. 11. Total annualized cost vs percent water usage allowed.

limited area scenario, where biomass is the least expensive option because it does not require energy storage. However, biomass is the only technology that requires water use. So as water use becomes more restricted, the energy demand must be met through other options.

Since the other generating technologies do not require water use, the model is free to choose any of these options to replace biomass as the allowed water use is reduced. The wind turbines are less expensive per energy output than both solar panel options, so the model chooses to mostly utilize this option to meet the energy demand. However, relying on one generating technology would have required more energy storage. By diversifying to include solar panels with the wind turbines, the low wind periods can be supplemented by solar energy, reducing the need for large and expensive storage systems.

5. Conclusion

A literature gap has been identified regarding comprehensive studies holistically addressing energy-water-land nexus considerations for the design of renewable energy systems.

The proposed framework can address this gap by analyzing renewable energy data in terms of wind speeds, solar irradiance and biomass resource consumption, along with regional factors and perspectives in a combined MILP model. Local restrictions regarding water and land use can be taken into consideration to incorporate the environmental impact of solution strategies, and explore trade-offs between water, energy, land and cost.

The developed model framework can easily be adjusted to various regions by modifying the specified input data and restrictions. Therefore, the key contributions of this work are:

 Development of detailed optimization models of key technological components of energy systems that include water and land interactions.

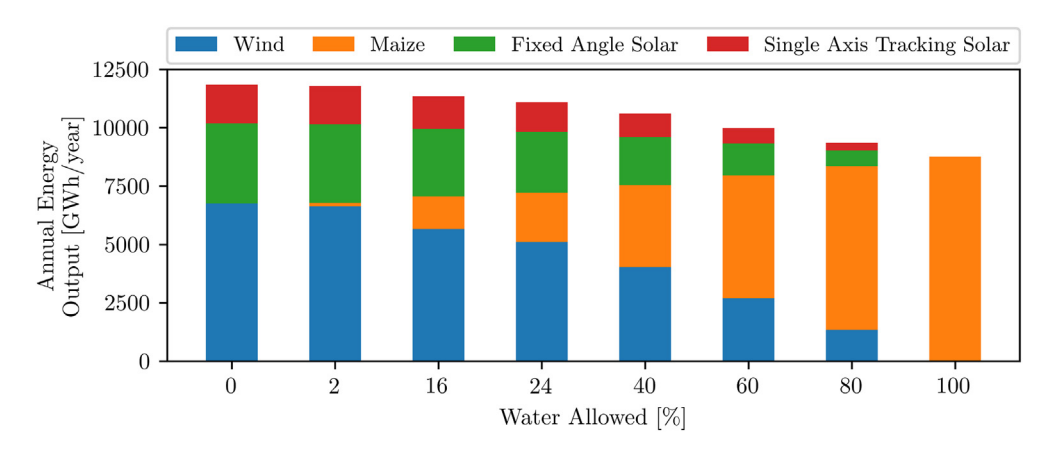


Fig. 12. Technology allocations at varying percentages of allowed water use.

- · Development of a holistic integrated optimization model for infrastructure planning of energy systems, that takes as input detailed key compo-
- · Development of a multi-objective optimization solution approach for energy-water-land nexus trade-off analysis.

Additionally, the presented case study demonstrates that a multi-scale multi-objective approach to optimizing renewable energy generation and storage systems is essential for considering all of the relevant factors involved in future energy infrastructure planning decisions. The results also underline the significance of geographic factors and resource availability on the transition towards renewable energy generation. Future work can expand on including more technology options, e.g. add switchgrass as an additional biomass option or analyze various options regarding solar panel and inverter combinations. Further, the applied surrogate models can be replaced by taking into account more technology-specific factors. Ultimately, the proposed model can also be applied for a different region with adjusted objectives.

Abbreviations

CAES	compressed air energy storage
GHG	global greenhouse gas
MILP	mixed-integer linear program
MINLP	mixed-integer nonlinear program
PHS	pumped hydropower storage
SAT	single axis tracking

Parameters

$ u_{n, t}' $ $ u_{n, t}^{0} $	wind speed at day n and time t at hub height of wind turbine measured wind speed at day n and time t	
ν^{ci}	cut in speed of wind turbine	
$ u^{co}$	cut out speed of wind turbine	
ν^n	nominal speed of wind turbine	
$\nu_{r, n, t}$	wind speed at day n and time t at hub height of wind turbine in row r	
A ^{sol, fixed}	area required per energy output of fixed solar panels (ha/kWh/year)	
$A^{sol, SAT}$	area required per energy output of fixed solar panels (ha/kWh/year)	
A_{panel}	surface area os a single solar panel	
A_{rot}	rotor area of wind turbine	
b	intercept of wind speed vs. power output correlation	
C^L	cost of land occupied by a single turbine	
$capex_k^c$	capital cost of storage technology k for capacity	
$capex_k^p$	capital cost of storage technology k for power rating	
D	rotor diameter of wind turbine	
f_{NREL}	solar panel cost factor including all cost except land cost	
JNREL H	hub height of wind turbine	
int _i	Y-intercept of piecewise section, power output wind farm vs.	
шиј	area	
L^{panel}	width of solar panel	
$L^{spacing}$	necessary distance between two neighboring solar panels	
M	big M constraint	
m	slope of wind speed vs. power output correlation	
P	capacity of a single solar panel	
p^n	nominal power output of a single wind turbine	
P P ^{demand}	power demand to be satisfied by the wind farm	
$p_t^{scale_g}$	fixed scaled power output of generating technology g in time t	
Pt P ^{target}	target constant power output	
pd	power demand to be satisfied	
PO	power output of a single solar panel	
pog, t	solar, wind, and maize power output at individual scale at time t	
R	rotor radius of wind turbine	

Sets	
С	column index for wind turbine placing
GB	gearbox options of wind turbine, GB = {Three - Stage
	Planetary/Helical, Single - Stage Drive with Medium -
	Speed Generator, Multi – Path Drive with Multiple Generators,
	Direct Drive}
GEN	generator options of wind turbine, $GEN = \{Three - Stage Drive \}$
	with High - Speed Generator, Single - Stage Drive with Me-
	dium - Speed and Permanent - Magnet Generator, Multi -
	Path Drive with Permanent — Magnet Generator, Direct Drive}
G	generating technologies, $G = \{\text{solar fixed angle, solar single axis}\}$
	tracking, biomass, wind}
I	piecewise section, wind speed vs. power, $I = \{i1, i2, i3\}$
J	piecewise sections, area vs. power, $J = \{j1, j2\}$
K	storage technologies, $K = \{PHS, CAES\}$
N	representative days in time horizon, $N = \{1,2,3,4\}$
R	row index for wind turbine placing
T	hours in time horizon, $T = \{t1,, t8760\}$
U	cost contributors of a single wind turbine, $U = \{blade, hub, ab, blade, blade$
	pitch, nose, shaft, bearing, brake, elec, yaw, cool, nac, safety,
	tower, found, int, gearbox, gen, main, platform, trans, road, in-
	stall, permit}
X	inverter and solar panel combinations

maximum area use to energy output ratio

maximum water use to energy output ratio

area between wind turbines

years of expected lifespan of technologies G and K

slope of piecewise section, power output wind farm vs. area

Variables

 κ_k

ratioae

ratiowe

 $slope_i$ T^{lifespan}

 x^2

re _K	capacity of storage technology is
κ_{plant}	capacity of solar farm
ф	azimuth angle of solar panel
θ	tilt angle of solar panel
\boldsymbol{A}	area
A^{dife}	effective area difference between wind and maize
A^{dif}	area difference between wind and maize
A^{maize}	area required for biomass farming
A^{solar}	area required for fixed and SAT solar panel systems
A^{total}	total area of all generating technologies
A^{wind}	area required for wind turbines
C^{emp}	overall cost of a single wind turbine (empirical correlations)
C^{inv}	investment cost
C^{land}	cost of land
C^{maize} , op	operating cost of biomass system
C^{op}	operating cost
C^{panels}	cost of solar panels
C^{P}	cost of a single solar panel
C^{total}	overall cost
$C^{turbine}$	cost of wind turbines
C_k	cost of storage technology k
$C_{biomass}$	cost of biomass
C_{solar}	cost of solar farm (single axis tracking and fixed angle)
C_{wind}	cost of wind farm
f_i , c , r , n ,	t auxiliary wind speed for piecewise linear correlation, wind
speed vs.	power output of wind turbine
N	number of solar panels
$N^{turbine}$	number of wind turbines
N_c	number of wind turbines in all columns at row 1
N_r	number of wind turbines in all rows at column 1

capacity of storage technology k

 $P_{p}^{bal}k$ power in storage technology k at time t

 P_t^{gen} generated power in time t

 p^{max} , $scale^2$ maximum amount of maize output P_k^{rat} power rating of storage technology k

 P_k^{rat} power rating of storage technology k $P_k^{religse}$ power released from storage technology k in time t

 P_b k power released from storage technology k in time t power entered into storage technology k in time t

 P^{total} total energy output in time horizon p_g power output of generating technology g

pa_i piecewise power, area vs. energy

 po_c , r, n, t power output of a single wind turbine at time t on day n in position c, r

 $scale_{\alpha}$ number of solar panels, wind turbines, or area of maize

water^{max} maximum allowed water use

watertotal used water (m3/year)

 $y_c^{t,b\mu\nu}$ binary variable for wind turbine purchase at time t in position c, r

 y_{c}^{t} , \mathcal{V} , n, t binary variable for wind turbine operation at time t on day n in

position c, r

 y_m binary variable for maize land cost z_i piecewise binary, area vs. energy

 z_i , c, r, n, tpiecewise binary, wind speed vs. power output of wind turbine

CRediT authorship contribution statement

Julie Cook: Methodology, Software, Validation, Formal analysis, Data curation, Writing – original draft, Writing – review & editing, Visualization. Marcello Di Martino: Validation, Writing – original draft, Writing – review & editing. R. Cory Allen: Methodology, Software, Validation, Writing – review & editing, Supervision. Efstratios N. Pistikopoulos: Formal analysis, Writing – review & editing, Supervision, Project administration, Funding acquisition. Styliani Avraamidou: Conceptualization, Methodology, Software, Validation, Formal analysis, Writing – original draft, Writing – review & editing, Visualization, Supervision, Project administration.

Declaration of competing interest

The authors declare that they have no known competing financial interests or personal relationships that could have appeared to influence the work reported in this paper.

Acknowledgements

This work was supported by the National Science Foundation (Grant no. 1739977 [INFEWS]). The authors also gratefully acknowledge financial support from the University of Wisconsin-Madison, Texas A&M University, and Texas A&M Energy Institute.

References

- Ahmetovic, E., Martín, M., Grossmann, I.E., 2010. Optimization of energy and water consumption in corn-based ethanol plants. Ind. Eng. Chem. Res. 49, 7972–7982.
- Albrecht, T.R., Crootof, A., Scott, C.A., 2018. The water-energy-food nexus: a systematic review of methods for nexus assessment. Environ. Res. Lett. 13, 043002.
- Allen, R.C., Baratsas, S.G., Kakodkar, R., Avraamidou, S., Demirhan, C.D., Heuberger-Austin, C.F., Klokkenburg, M., Pistikopoulos, E.N., 2022. A multi-period integrated planning and scheduling approach for developing energy systems. Optim. Control Appl. Methods https://doi.org/10.1002/oca.2866 In press.
- Allen, R.C., Baratsas, S.G., Kakodkar, R., Avraamidou, S., Powell, J.B., Heuberger, C.F., Demirhan, C.D., Pistikopoulos, E.N., 2021. An optimization framework for solving integrated planning and scheduling problems for dense energy carriers. IFAC-PapersOnLine 54 (3), 621–626. https://doi.org/10.1016/j.ifacol.2021.08.311 In press.
- Allen, R.C., Nie, Y., Avraamidou, S., Pistikopoulos, E.N., 2019. Infrastructure planning and operational scheduling for power generating systems: an energy-water nexus approach. In: Muñoz, S.G., Laird, C.D., Realff, M.J. (Eds.), Proceedings of the 9th International Conference on Foundations of Computer-aided Process Design. volume 47 of Computer Aided Chemical Engineering. Elsevier, pp. 233–238. https://doi.org/10.1016/B978-0-12-818597-1.50037-0 URL: https://www.sciencedirect.com/science/article/pii/B9780128185971500370.

- Attias, K., Ladany, S., 2011. Optimal layout for wind turbine farms. World Renewable Energy Congress 2011 Sweden, pp. 4153–4160 https://doi.org/10.3384/ecp110574153.
- Avraamidou, S., Beykal, B., Pistikopoulos, I.P., Pistikopoulos, E.N., 2018a. A hierarchical food-energy-water nexus (few-n) decision-making approach for land use optimization. Computer Aided Chemical Engineering, vol. 44. Elsevier, pp. 1885–1890.
- Avraamidou, S., Milhom, A., Sarwar, O., Pistikopoulos, E.N., 2018b. Towards a quantitative food-energy-water nexus metric to facilitate decision making in process systems: a case study on a dairy production plant. Computer Aided Chemical Engineering. vol. 43. Elsevier, pp. 391–396.
- Avraamidou, S., Baratsas, S.G., Tian, Y., Pistikopoulos, E.N., 2020. Circular economy-a challenge and an opportunity for process systems engineering. Comput. Chem. Eng. 133, 106629
- Baratsas, S.G., Pistikopoulos, E.N., Avraamidou, S., 2021. A systems engineering framework for the optimization of food supply chains under circular economy considerations. Sci. Total Environ. 794, 148726.
- Baratsas, S.G., Pistikopoulos, E.N., Avraamidou, S., 2022. A quantitative and holistic circular economy assessment framework at the micro level. Comput. Chem. Eng., 107697 https://doi.org/10.1016/j.compchemeng.2022.107697.
- Beykal, B., Avraamidou, S., Pistikopoulos, I.P., Onel, M., Pistikopoulos, E.N., 2020. Domino: data-driven optimization of bi-level mixed-integer nonlinear problems. J. Glob. Optim. 78, 1–36.
- Biegler, L.T., Lang, Y.d., 2012. Multi-scale optimization for advanced energy processes. Computer Aided Chemical Engineering. vol. 31. Elsevier, pp. 51–60.
- Bogdanov, D., Ram, M., Aghahosseini, A., Gulagi, A., Oyewo, A.S., Child, M., Caldera, U., Sadovskaia, K., Farfan, J., De Souza Noel Simas Barbosa, L., Fasihi, M., Khalili, S., Traber, T., Breyer, C., 2021. Low-cost renewable electricity as the key driver of the global energy transition towards sustainability. Energy 227, 120467. https://doi.org/10.1016/j. energy.2021.120467.
- Boretti, A., Rosa, L., 2019. Reassessing the projections of the world water development report. npj Clean Water 2, 1–6.
- Braun, R., Weiland, P., Wellinger, A., 2010. Biogas from energy crop digestion. IEA Bioenergy.
 Chen, Z., Avraamidou, S., Liu, P., Li, Z., Ni, W., Pistikopoulos, E.N., 2021. Optimal design of integrated urban energy systems under uncertainty and sustainability requirements.
 Comput. Chem. Eng. 155, 107502.
- Demirhan, C.D., Tso, W.W., Powell, J.B., Pistikopoulos, E.N., 2021. A multi-scale energy systems engineering approach towards integrated multi-product network optimization. Appl. Energy 281, 116020. https://doi.org/10.1016/j.apenergy.2020.116020 URL: https://www.sciencedirect.com/science/article/pii/S0306261920314604.
- Di Martino, M., Avraamidou, S., Pistikopoulos, E., 2020. Superstructure optimization for the design of a desalination plant to tackle the water scarcity in Texas (USA). In: Pierucci, S., Manenti, F., Bozzano, G.L., Manca, D. (Eds.), 30th European Symposium on Computer Aided Process Engineering. volume 48 of Computer Aided Chemical Engineering. Elsevier, pp. 763–768. https://doi.org/10.1016/B978-0-12-823377-1.50128-2 URL: https://www.sciencedirect.com/science/article/pii/B9780128233771501282.
- Di Martino, M., Avraamidou, S., Cook, J., Pistikopoulos, E.N., 2021. An optimization framework for the design of reverse osmosis desalination plants under food-energy-water nexus considerations. Desalination 503, 114937. https://doi.org/10.1016/j.desal.2021. 114937 URL: https://www.sciencedirect.com/science/article/pii/S0011916421000084.
- Di Martino, M., Avraamidou, S., Pistikopoulos, E.N., 2022. A neural network based superstructure optimization approach to reverse osmosis desalination plants. Membranes 12 (2), 199. https://doi.org/10.3390/membranes12020199 URL: https://www.mdpi.com/ 2077-0375/12/2/199.
- Drews, M., Larsen, M.A.D., Peña Balderrama, J.G., 2020. Projected water usage and land-use-change emissions from biomass production (2015–2050). Energy Strategy Rev. 29, 100487. https://doi.org/10.1016/j.esr.2020.100487 URL: https://www.sciencedirect.com/science/article/pii/S2211467X20300407.
- Energy Reliability Council of Texas, 2018. Quick facts. URL http://www.ercot.com/content/wcm/lists/144926/ERCOT_Quick_Facts_41018.pdf.
- Fingersh, L., Hand, M., Laxson, A., 2006. Wind turbine design cost and scaling model. URL https://www.nrel.gov/docs/fy07osti/40566.pdf.
- Finley, J.W., Seiber, J.N., 2014. The nexus of food, energy, and water. J. Agric. Food Chem. 62, 6255–6262. https://doi.org/10.1021/jf501496r.
- Fu, R., Feldman, D., Margolis, R., 2018. U.S. Solar Photovoltaic System Cost Benchmark: Q1 2018. URL https://www.nrel.gov/docs/fy19osti/72399.pdf.
- Gao, J., Xu, X., Cao, G., Ermoliev, Y.M., Ermolieva, T.Y., Rovenskaya, E.A., 2021. Strategic decision-support modeling for robust management of the food-energy-water nexus under uncertainty. J. Clean. Prod. 292, 125995. https://doi.org/10.1016/j.jclepro.2021.125995 URL: https://www.sciencedirect.com/science/article/pii/S0959652621002158.
- Garcia, D.J., You, F., 2015. Life cycle network modeling framework and solution algorithms for systems analysis and optimization of the water-energy nexus. Processes 3, 514–539.
- Garcia, D.J., You, F., 2016. The water-energy-food nexus and process systems engineering: a new focus. URL: https://www.sciencedirect.com/science/article/pii/S0098135416300552Comput. Chem. Eng. 91, 49–67. https://doi.org/10.1016/j.compchemeng.2016.03.003 12th International Symposium on Process Systems Engineering & 25th European Symposium of Computer Aided Process Engineering (PSE-2015/ESCAPE-25), 31 May 4 June 2015, Copenhagen, Denmark.
- Garcia, D., You, F., 2017. Systems engineering opportunities for agricultural and organic waste management in the food-water-energy nexus. Curr. Opin. Chem. Eng. 18, 23–31.
- Gu, D., Andreev K, D.M., 2021. Major trends in population growth around the world. China CDC Wkly 3, 604–613. https://doi.org/10.46234/ccdcw2021.160.
- Holmgren, W.F., Hansen, C.W., Mikofski, M.A., 2018. pvlib python: a python package for modeling solar energy systems. J. Open Source Softw. 3 (29), 884. https://doi.org/10. 21105/joss.00884.
- Joskow, P.L., 2019. Challenges for wholesale electricity markets with intermittent renewable generation at scale: the US experience. URLOxford Rev. Econ. Policy 35, 291–331.

- $https://doi.org/10.1093/oxrep/grz001\ arXiv:https://academic.oup.com/oxrep/article-pdf/35/2/291/28504934/grz001.pdf.$
- Lambin, E.F., Meyfroidt, P., 2011. Global land use change, economic globalization, and the looming land scarcity. Proc. Natl. Acad. Sci. 108, 3465–3472.
- Lohrmann, A., Farfan, J., Caldera, U., Lohrmann, C., Breyer, C., 2019. Global scenarios for significant water use reduction in thermal power plants based on cooling water demand estimation using satellite imagery. Nat. Energy 4, 1040–1048.
- Lunik, E., Langemeier, M., 2015. International Benchmarks for Corn Production. Purdue Agriculture Center for Commercial Agriculture.
- Martín, M., Grossmann, I.E., 2015. Water-energy nexus in biofuels production and renewable based power. Sustain. Prod. Consum. 2, 96–108.
- Mohtar, R.H., Daher, B., 2019. Lessons learned: creating an interdisciplinary team and using a nexus approach to address a resource hotspot. Sci. Total Environ. 650, 105–110. https:// doi.org/10.1016/j.scitotenv.2018.08.406 URL: https://www.sciencedirect.com/science/ article/pii/S0048969718333825.
- Namany, S., Govindan, R., Martino, M.D., Pistikopoulos, E.N., Linke, P., Avraamidou, S., Al-Ansari, T., 2021. An energy-water-food nexus-based decision-making framework to guide national priorities in Qatar. Sustain. Cities Soc. 75, 103342. https://doi.org/10.1016/j.scs.2021.103342 URL: https://www.sciencedirect.com/science/article/pii/S2210670721006181.
- Nie, Y., Avraamidou, S., Xiao, X., Pistikopoulos, E.N., Li, J., 2019a. Two-stage land use optimization for a food-energy-water nexus system: a case study in Texas Edwards Region. In: Muñoz, S.G., Laird, C.D., Realff, M.J. (Eds.), Proceedings of the 9th International Conference on Foundations of Computer-aided Process Design. volume 47 of Computer Aided Chemical Engineering. Elsevier, pp. 205–210. https://doi.org/10.1016/B978-0-12-818597-1.50033-3.

- Nie, Y., Avraamidou, S., Xiao, X., Pistikopoulos, E.N., Li, J., Zeng, Y., Song, F., Yu, J., Zhu, M., 2019b. A food-energy-water nexus approach for land use optimization. Sci. Total Environ. 659, 7–19. https://doi.org/10.1016/j.scitotenv.2018.12.242 URL: https://www. sciencedirect.com/science/article/pii/S004896971835112X.
- Pappas, I., Avraamidou, S., Katz, J., Burnak, B., Beykal, B., Türkay, M., Pistikopoulos, E.N., 2021. Multiobjective optimization of mixed-integer linear programming problems: a multiparametric optimization approach. Ind. Eng. Chem. Res. 60 (23), 8493–8503. https://doi.org/10.1021/acs.iecr.1c01175.
- Sahinidis, N.V., 1996. Baron: a general purpose global optimization software package. J. Glob. Optim. 8, 201–205.
- Scanlon, B.R., Duncan, I., Reedy, R.C., 2013. Drought and the water–energy nexus in Texas. Environ. Res. Lett. 8, 045033.
- Tso, W.W., Demirhan, C.D., Heuberger, C.F., Powell, J.B., Pistikopoulos, E.N., 2020. A hierarchical clustering decomposition algorithm for optimizing renewable power systems with storage. Appl. Energy 270, 115190.
- United Nations, 2019. World Population Prospects 2019: Highlights. Department of Economic and Social Affairs, Population Division.
- Vakilifard, N., Anda, M., Bahri, P.A., Ho, G., 2018. The role of water-energy nexus in optimising water supply systems–review of techniques and approaches. Renew. Sustain. Energy Rev. 82, 1424–1432.
- Xu, C., Hao, C., Li, L., Han, X., Xue, F., Sun, M., Shen, W., 2018. Evaluation of the power-law wind-speed extrapolation method with atmospheric stability classification methods for flows over different terrain types. Appl. Sci. 8. https://doi.org/10.3390/app8091429 URL: https://www.mdpi.com/2076-3417/8/9/1429.